# ENERGY FOR ROCK BREAKAGE

Andreas Böhm, Roland Mayerhofer, Wolfgang Öfner

**Chair of Mineral Processing**
Department Mineral Resources Engineering, Montanuniversitaet Leoben
Franz-Josef-Straße 18, A-8700 LEOBEN, Austria
Tel.: +43(0)3842/402-1800,1801 Fax: +43(0)3842/402-1802
aufbereitung@unileoben.ac.at, www.unileoben.ac.at/mineralaufbereitung
UID: ATU 57480504

# CONTENT

# 1. INTRODUCTION

The design of mechanical comminution systems calls for a characterization of the comminution properties of minerals and rocks with respect to their individual breakage characteristics and the specific energy consumption as a function of the product dispersity, the latter to be described by the particle size distribution and the specific surface of the products. A test procedure named the "Optimized Comminution Sequence" (OCS) has been developed at the Chair of Mineral Processing at Montanuniversitaet Leoben for the purpose of determining the natural (i.e. equipment-independent) breakage characteristics (NBC) of brittle mineral matter together with the energy/surface relationship culminating in the Rittinger coefficient. The latter relates the creation of new surface to the net energy consumption. The particle size distributions of OCS products of the same material but of different top size display self-similarity and can often be linearized in a Gates-Gaudin-Schuhmann plot [1].

By the example of the OCS built up for the Less Fines project, the method for the determination of the comminution characteristics of mineral material is outlined. The comminution parameters of six different samples out of three European quarries are presented. The samples stem from the project partners Hengl-Bitustein (Austria, 1 sample, amphibolite); Cementos Portland (Spain, 1 sample, limestone); Nordkalk (Sweden, 4 samples of different types of limestones out of the quarry on Gotland).

# 2. THE CONCEPT OF THE OPTIMIZED COMMINUTION SEQUENCE (OCS)

At the Chair of Mineral Processing at Montanuniversitaet Leoben, Austria, a laboratory method for mechanical fragmentation was developed that obeys the principles of the energy optimized comminution.

It consists of a succession of numerous comminution stages in closed circuit design to guarantee a small size reduction ratio. The settings of the apparatus of each stage are optimally adapted to the specific size reduction step.

The circuit design of "closed circuit with prescreening" (Figure 1) is simulated in the laboratory by cyclic comminution tests at a high circulating load of at least 100%. Each cycle ends with intermediate classification at a defined screen aperture. Within each circuit, mechanical screening is replaced by manual screening, which is still the most accurate laboratory method of particle size separation in the particle size range 0.04-100 mm.

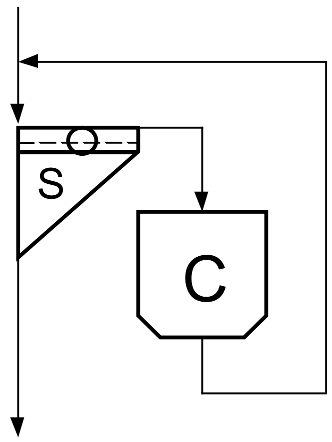


**Figure 1: Scheme of the closed circuit design with prescreening.
S ... screening, C ... comminution**

The objective of energy efficient mechanical comminution is to fragment a set of particles of a given maximum size and a known size distribution to a defined lower maximum particle size at the minimum amount of supplied energy. The energy consumption is directly correlated to the amount of fines. An overproduction of fine material reflects the waste of energy.

The already produced fine material present in the comminution tool causes energy dissipation by compaction. Prescreening serves to separate the existing fines in the feed, thus directing the energy supplied by the comminution tool to the coarse particles. The accurate (manual) intermediate screening removes the fine particles soon after their creation. High circulating load causes a short retention time of the particles within the comminution tool resulting in a smaller number of stress events per particle and cycle.

The net energy consumption and the specific surface of selected particle size classes of the comminution product are measured at each stage as well as the particle size distribution of the feed and the comminution product.

According to the experience accumulated in mineral processing, this method delivers the comminution product with a particle size distribution characterized by the smallest variation of particle sizes at a given maximum particle size independently from the used machinery.

There is no technical process of mechanical multi-particle fragmentation known to produce a smaller amount of fines of a given material. Therefore this particle size distribution is regarded as a material’s characteristic called the Natural Breakage Characteristic (NBC).

The measurement of the net energy consumption for the comminution of the oversize material at each stage as well as the determination of the specific surface of the comminution products provide the data to construct the energy register diagram.

According to Prof. H.J. Steiner the energy register is defined as the minimum amount of energy that has to be expended per mass unit for the comminution from the entirely unfragmented state to the desired maximum particle size. Vice versa the difference between two energy registers delivers the specific energy consumption (refer to Figure 2).

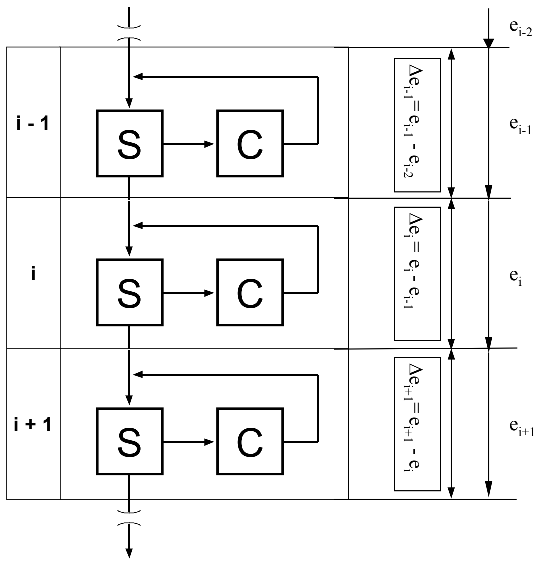


**Figure 2: General representation of the principle of energy optimized comminution according to Steiner [2]**

To obtain the energy register function the accumulated specific energy consumption is plotted versus the specific surface of the assigned product.

If the measured data set can be approximated by a linear function, then the inclination is known as the Rittinger coefficient. The NBC and the Rittinger coefficient are machinery independent material's parameters apt for the characterization of the comminution behaviour of a given raw material. The particle shape factor and the minimum particle size of mechanical fragmentation complete the set of material parameters.

According to the experience accumulated at the Chair of Mineral Processing, the measured values from the stage-wise optimized comminution confirm Peter Ritter von Rittinger's hypothesis of proportionality between energy consumption and new developed specific surface. In the case of not energy optimized comminution, the plot of the mass specific surface of the comminution products versus the accumulated energy consumption is characterized by a curve of decreasing inclination (Figure 3). Thus Rittinger's hypothesis represents the limiting case of an energy-optimized comminution, which can be approximated by the method of OCS. The coefficient of proportionality usually ranges from 10 to 150 cm²/J for mineral raw material.

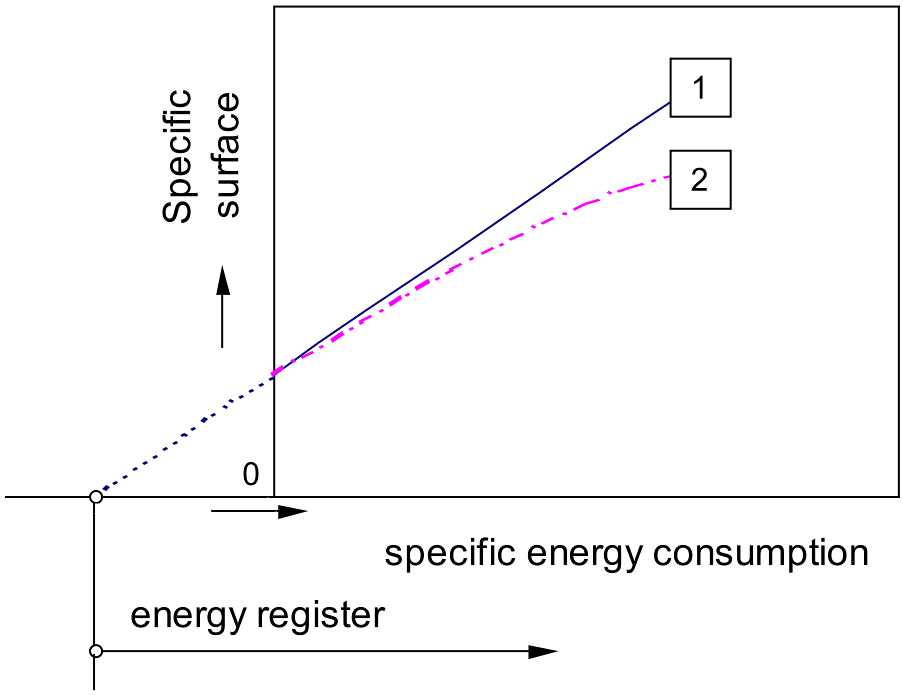


**Figure 3: Energy register functions for**
**1 … the energy optimized comminution by OCS**
**2 … not energy optimized (technical) comminution**

## 3. SAMPLE MASS

The feed to the OCS in the Less Fines project consisted of 10 to 20 blocs of a maximum size of 200 mm. They were supplied by the Chair of Mining Engineering, Montanuniversitaet Leoben. Most of the blocs represent the remaining material after cylinder drilling. For the total mass of the treated samples refer to Table 1.

**Table 1: Original sample mass supplied to the primary crusher**

| | Hengl-Bitustein | Cementos Portland | Nordkalk | | | |
|---|---|---|---|---|---|---|
| | | | F | S | R | K |
| sample mass [kg] | 262 | 421 | 368 | 347 | 314 | 365 |

According to the measurements of specific gravity (refer to Table 5) of the particle size classes -100 +40 µm and –40 µm, all the samples turned out to be homogeneous in their mineralogical composition.

# 4. EQUIPMENT AND TEST PROCEDURE

The Optimized Comminution Sequence built up for the Less Fines project consists of three crushing stages and two grinding stages. The pre- and intermediate screening to simulate the closed circuit was done manually at the apertures 40 mm, 16 mm, 6.3 mm, 3.15 mm and 1 mm (compare to Figure 4).

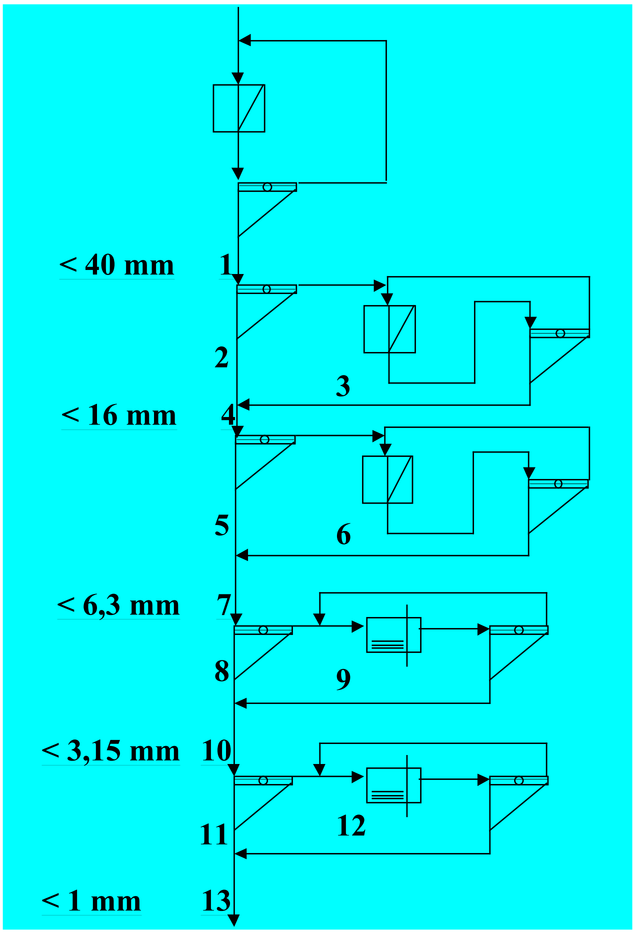


**Figure 4: Flowsheet of the Optimized Comminution Sequence built up for the Less Fines Project**

# 4.1. EQUIPMENT

A laboratory jaw crusher at Maschinenfabrik Liezen (MFL) about 70 km north of Leoben was rented to crush the blocs of a size of 200 mm in the first comminution stage. All the other comminution tools belong to the standard testing equipment of the chair.

For technical data and pictures of the utilized apparatus refer to Figures 5 to 12.

## 1st crushing stage

JAW CRUSHER, MFL / Liezen

**Figure 5: Front view**

**Figure 6: View into the mouth, both jaws are grooved down to the discharge**

Type: STE 50 / 30

| | | |
|---|---|---|
| cycles/sec: | 3.3 | $s^{-1}$ |
| installed power: | 35 | kW |
| dimensions of the mouth: | | |
| gape: | 0.500 | m |
| breadth: | 0.280 | m |
| closed side setting: | | |

adjusted to a circulating load of 100% at a screen aperture of 0.04 m

## $2^{nd}$ crushing stage

LABORATORY - JAW CRUSHER: Retsch BB 200/Mangan


cycles/sec: 4.6 $s^{-1}$

installed power: 1.5 kW

dimensions of the mouth:

gape: 0.14 m

breadth: 0.14 m

closed side setting:

adjusted to a circulating load of 100% at a screen aperture of 0.016 m

**Figure 7: Front view**

**Figure 8: View into the mouth**

## 3rd crushing stage

LABORATORY - JAW CRUSHER: Fuchs BB 150

| | | |
|---|---|---|
| cycles/sec: | 3.4 | $s^{-1}$ |
| installed power: | 1.3 | kW |
| dimensions of the mouth: | | |
| gape: | 0.12 | m |
| breadth: | 0.15 | m |
| closed side setting: | 0.005 | m |
| open side setting: | 0.025 | m |
| screen aperture: | 0.0063 | m |

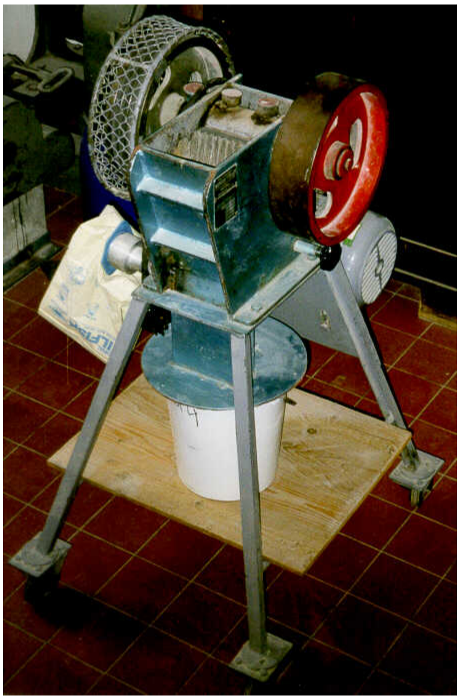

**Figure 9: Front view**

**Figure 10: View into the mouth**

## Both grinding stages

TUMBLING MILL

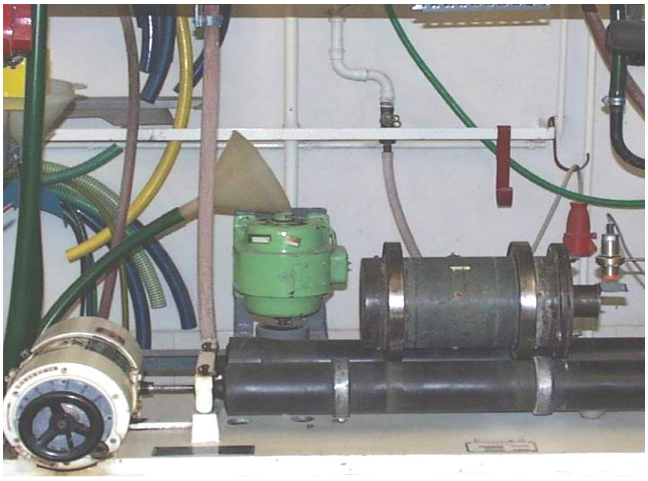

Figure 11: Test rig of the rod mill consisting of the roller drive, the rod mill and the revolution counter

mill diameter: 0.154 m

mill length: 0.300 m

grinding media:

steel rods

number: 9

mass: 8 kg

degree of filling: 30 vol.%

:

Figure 12: View into the mill

mill speed "n":

$n = 0.6 – 0.7\ n_c$

$n_c$ … critical speed

## 4.2. TEST PROCEDURE

The cyclic comminution test procedure is outlined by the example of the first crushing stage. The crusher setting was adjusted to a circulating load of 100%. After crushing, the comminution product was screened manually (Figure 13). The oversize was recycled to the crusher (Figure 14), the undersize was stored for the following screen analysis. The first comminution stage was the only, in which energy measurement was not possible.

**Figure 13: Intermediate screening**

**Figure 14: Feeding the crusher**

The reduction of the sample mass to obtain the input for the screen analyses followed the strict rules of sampling. Coning and quartering served for sample splitting in the first stage (100% -40 mm); a riffle sample splitter was used in the size range between 16 and 3.15 mm; below 1 mm a rotary sample splitter provided the desired partition. From the smallest particle size classes (-100 +40 and -40 µm) the specific gravity and the volume specific surface were determined.

Except of the first comminution stage, the feed sample was reconstituted from the size classes of the previous screen analyses by means of mass equivalent mixture. The closed side settings in the crushing stages are listed in Table 2. The settings of the laboratory rod mill can be found on page 9.

Differing from all the other comminution stages (circulating load 100%), the circulating load within the third stage varied between 200 and 250%.

**Table 2: Adjustments of the closed side setting of the crushers**

| comminution stage | mesh size | closed side setting (CSS) of the crushers [mm] | | | | | |
|---|---|---|---|---|---|---|---|
| | | Hengl- | Cementos | Nordkalk | | | |
| | [mm] | Bitustein | Portland | F | S | R | K |
| 100% -40 mm | 40 | 34 | 45 | 41 | 35 | 33.5 | 36 |
| 100% -16 mm | 16 | 20 | 18.5 | 18 | 17 | | 20.5 |
| 100% -6.3 mm | 6.3 | 5 | 5 | 5 | 5 | 5 | 5 |

Table 3 lists the size reduction ratios defined as the quotient of the $k_{80}$-values of the feed and the product.

**Table 3: Size reduction ratios**

| comminution stage | size reduction ratio | Hengl-Bitustein | Cementos Portland | Nordkalk | | | |
|---|---|---|---|---|---|---|---|
| | | | | F | S | R | K |
| 100% -40 mm | $k_{80,200}$ / $k_{80,40}$ | 5.45 | 5.55 | 5.51 | 5.43 | 5.42 | 5.49 |
| 100% -16 mm | $k_{80,40}$ / $k_{80,16}$ | 2.54 | 2.51 | 2.53 | 2.59 | 2.59 | 2.53 |
| 100% -6.3 mm | $k_{80,16}$ / $k_{80,6.3}$ | 2.70 | 2.73 | 2.76 | 2.70 | 2.71 | 2.76 |
| 100% -3.15 mm | $k_{80,6.3}$ / $k_{80,3.15}$ | 2.18 | 2.07 | 2.06 | 2.07 | 2.06 | 2.08 |
| 100% -1 mm | $k_{80,3.15}$ / $k_{80,1}$ | 3.17 | 3.09 | 3.12 | 3.11 | 3.12 | 3.07 |

# 5. MEASUREMENT OF THE ENERGY CONSUMPTION

Starting with the second stage the energy consumption of the different comminution tools was measured.

## 5.1. LABORATORY JAW CRUSHERS

A digital multimeter served to measure and record the true power consumption in a standard electric circuit for symmetric load. The voltage was taken between the outer and the neutral conductor. The multimeter (type M 4660M, Voltcraft) was connected to a PC via the RS 232 interface.

**Figure 15: Circuit for measuring the true power consumption at the laboratory jaw crushers**

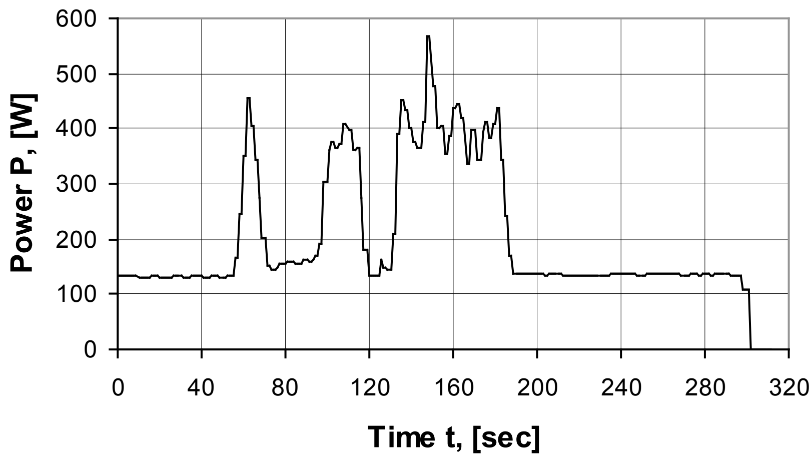


**Figure 16: Plot of true power consumption versus time**

In general, the net energy consumption of such a circuit design is defined by equation 1,

$$E_{Ne} = 3\int_{t1}^{t2} (P_{Br}(t) - \overline{P_L})dt \qquad \text{equ. 1}$$

$E_{Ne}$ ... mean net energy consumption

$P_{Br}$ ... total power draw

$\overline{P_L}$ ... mean power draw on no-load

$t_1$, $t_2$ ... time of beginning and end

Due to the time base of data transmission of 1 s and the circuit design, the calculation of the net energy consumption could be simplified to equation 2,

$$E_{Ne} = 3\sum_{i=0}^{n} (P_{ti,Br} - \overline{P}_L) \qquad \text{equ. 2}$$

$\overline{P}_{ti,Br}$ ... total power draw at time "i" by one conductor

$\overline{P_L}$ ... mean power draw on no-load

For the calculation of the mean idle power draw refer to equation 3,

$$\overline{P_L} = \frac{\overline{P}_{vor} + \overline{P}_{nach}}{2} \qquad \text{equ. 3}$$

$\overline{P_L}$ ... mean idle power draw

$\overline{P}_{vor}$ ... mean power draw on no-load before crushing

$\overline{P}_{nach}$ ... mean power draw on no-load after crushing

The results of the electronic measurement were controlled by synchronous measurement of the power draw with an electricity supply meter: the deviation between the two independent systems on no-load was < 0.5% and on load < 4%. The higher value on load is caused by the restrictions on manual time measurement involved with the electricity meter.

Further calculations used were the arithmetic mean of the measurements of all the cycles.

## 5.2. TUMBLING MILL

In contrast to a crusher, the net power draw of a tumbling mill remains constant. The relationship in equation 4, derived by Prof. H.J. Steiner [3], serves to calculate the net power draw.

$$E = c_p \cdot M_k \cdot g \cdot D \cdot U \qquad \text{equ. 4}$$

$c_P$ ... power number

$M_k$ ... mass of grinding media

g ... gravity acceleration

D ... mill diameter

U ... number of revolutions

From a series of calibration measurements the power number of the laboratory rod mill had been determined as 1.2.

# 6. DETERMINATION OF THE DISPERSITY OF THE COMMINUTION PRODUCTS

## 6.1. PARTICLE SIZE DISTRIBUTION

Manual screen analysis was conducted after mechanical prescreening on a laboratory test sieve shaker (Figure 17).

**Figure 17: Prescreening on a test sieve shaker, completed by manual screening**

The selected screens (DIN 4188, wire mesh) comprise the screen apertures 40 mm, 32 mm, 25 mm, 20 mm, 16 mm, 10 mm, 6.3 mm, 3.15 mm, 1 mm, 0.5 mm, 0.2 mm, 0.1 mm, and 0.040 mm. The particle size class -100 +40 µm of all the comminution products was purified by air jet screening.

## 6.2. SPECIFIC SURFACE AREA

Based on Kozeny's equation on the gas flow through a particle bed, the specific surface of a particle set can be determined by permeametry. Especially for the new created surface from grinding, the quite simple apparatus based on Blaine's method (constant volume) and the Permeran by Outokumpu (constant pressure) provide an easy to handle means for particle surface measurement.


**Figure 18: Photographs of the Permaran Outokumpu (left); and the Blaine apparatus manufactured by Tonindustrie Prüftechnik (right)**

The dispersity of the particle size class -40 µm and the purified size class -100 +40 µm of the comminution products (streams 1, 3, 6, 9, 12 in Figure 4) was determined. The data given in Table 4 represent the arithmetic mean of four measurements each, the standard deviation being less than 5%. The data form the base for the calculation of the specific surface of the comminution product according to GGS theory.

**Table 4: Measurement results of the volume specific surface**

| | | Volume Specific Surface | | | | |
|---|---|---|---|---|---|---|
| Sample | Particle Size Class | 100 % -40 mm (Stream 1) | 100 % -16 mm (Stream 3) | 100 % -6.3 mm (Stream 6) | 100 % -3.15 mm (Stream 9) | 100 % -1 mm (Stream 12) |
| | [µm] | [cm²/cm³] | [cm²/cm³] | [cm²/cm³] | [cm²/cm³] | [cm²/cm³] |
| LF 1 Hengl-Bitutstein | -100 +40 | 1566 | 1650 | 1586 | 1566 | 1475 |
| | -40 | 10416 | 11924 | 12068 | 10152 | 9100 |
| LF 2 Cementos Portland | -100 +40 | 1610 | 1685 | 1683 | 1796 | 1601 |
| | -40 | 15019 | 14826 | 17399 | 15557 | 16438 |
| LF 3 Nordkalk Type R | -100 +40 | 1563 | 1683 | 1448 | 1661 | 1452 |
| | -40 | 13802 | 13380 | 13934 | 12998 | 13969 |
| LF 4 Nordkalk Type S | -100 +40 | 1776 | 2096 | 2079 | 1902 | 1800 |
| | -40 | 13916 | 13514 | 12501 | 11646 | 11512 |
| LF 5 Nordkalk Type K | -100 +40 | 1888 | 1999 | 1773 | 1689 | 1431 |
| | -40 | 13410 | 15865 | 16691 | 11893 | 12417 |
| LF 6 Nordkalk Type F | -100 +40 | 1558 | 1636 | 1621 | 1552 | 1562 |
| | -40 | 12225 | 13442 | 12954 | 12009 | 11689 |

## 6.3. SPECIFIC GRAVITY

The specific gravity of particle size classes was measured by a He gas pycnometer, type Accu Pyk 1330 (Figure 19).


**Figure 19: The Accu Pyk 1330 at the Chair of Mineral Processing**

**Table 5: Measurement results of the specific gravity of selected particle size classes**

| | | Specific gravity | | | | | |
|---|---|---|---|---|---|---|---|
| Sample | Particle size class | 100 % -40 mm (stream 1) | 100 % -16 mm (stream 3) | 100 % -6.3 mm (stream 6) | 100 % -3.15 mm (stream 9) | 100 % -1 mm (stream 12) | arithmetic mean |
| | [µm] | [g/cm³] | [g/cm³] | [g/cm³] | [g/cm³] | [g/cm³] | [g/cm³] |
| LF 1 Hengl-Bitutstein | -10000 +6300 | 3.012 | - | - | - | - | 3.06 |
| | -3150 +1000 | 3.004 | - | - | - | - | |
| | -500 +200 | 3.002 | - | - | - | - | |
| | -100 +40 | 3.054 | 3.049 | 3.049 | 3.050 | 3.069 ; 3.064 | |
| | -40 | 3.051 | 3.082 | 3.097 | 3.098 | 3.103 ; 3.101 | |
| LF 2 Cementos Portland | -100 +40 | 2.717 | 2.716 | 2.718 | 2.726 | 2.720 | 2.72 |
| | -40 | 2.712 | 2.705 | 2.730 | 2.732 | 2.726 | |
| LF 3 Nordkalk Type R | -100 +40 | 2.718 | 2.727 | 2.716 | 2.710 | 2.716 | 2.72 |
| | -40 | 2.728 | 2.736 | 2.720 | 2.725 | 2.697 | |
| LF 4 Nordkalk Type S | -100 +40 | 2.721 | 2.723 | 2.726 | 2.726 | 2.720 | 2.73 |
| | -40 | 2.745 | 2.731 | 2.732 | 2.735 | 2.731 | |
| LF 5 Nordkalk Type K | -100 +40 | 2.740 | 2.735 | 2.727 | 2.734 | 2.706 | 2.73 |
| | -40 | 2.750 | 2.753 | 2.744 | 2.744 | 2.714 | |
| LF 6 Nordkalk Type F | 100/40 | 2.728 | 2.723 | 2.727 | 2.724 | 2.732 | 2.74 |
| | < 40 | 2.752 | 2.764 | 2.745 | 2.751 | 2.745 | |

Each value in Table 5 represents the arithmetic mean of three measurements. The standard deviation does not exceed 0.3%.

# 7. EVALUATION OF DATA

## 7.1. PARTICLE SIZE DISTRIBUTION AND MASS BALANCE

All the particle size distributions, represented by cumulative curves, are plotted into the GGS grid, which is commonly known to linearize products out of closed circuit design. The results of the air-jet screening of the particle size class -100 +40 µm were used to correct the measurement results of manual screening. The cumulative curves served to derive the mass split due to prescreening at each comminution stage starting with the comminution product of stream no. 1 (Figure 4).

## 7.2. SPECIFIC SURFACE OF THE COMMINUTION PRODUCTS

From the measured volume specific surface of the particle size class -100 +40 µm (refer to Table 4) the shape factor was calculated from GGS-theory (equations 5 to 7):

$$k_{ä} = \left(\frac{1}{n} - 1\right) \cdot \frac{D_o - D_u}{\frac{D_u}{k_u} - \frac{D_o}{k_o}}$$

equ. 5

$$n = \frac{\lg \frac{D_o}{D_u}}{\lg \frac{k_o}{k_u}}$$

equ. 6

| | |
|---|---|
| $k_{ä}$ ... | surface equivalent particle size |
| n ... | GGS-modulus of the particle size class |
| $D_o$, $D_u$ ... | cumulative passing at the upper and lower particle size limit |
| $k_o$, $k_u$ ... | upper and lower particle size limit |

The shape factor is assumed to remain constant for all the size classes. Within the calculations the arithmetic mean of five independent values (stream 1, 3, 6, 9, 12) was used. The weighted sum of the measured specific surface of the size classes -40 µm and -100 +40 µm make up at least 90% of the total specific surface.

**Table 6: Shape factors used for the calculation of the volume specific surface of the comminution product**

| Shape Factor [1] | | | | | |
|---|---|---|---|---|---|
| LF 1 Hengl-Bitustein | LF 2 Cementos Portland | LF 3 Nordkalk Type R | LF 4 Nordkalk Type S | LF 5 Nordkalk Type K | LF 6 Nordkalk Type F |
| 10.1 | 10.6 | 9.78 | 12.1 | 11.0 | 9.94 |

The surface of the remaining classes is calculated from their surface equivalent particle size and the shape factor:

$$f = a_v \cdot k_ä \quad \text{equ. 7}$$

The sum of the specific surface of all the size classes weighted by mass represent the total specific surface of the comminution product.

## 7.3. ENERGY REGISTER FUNCTION

For every complete comminution stage including prescreening, the measured mass specific energy consumption has to be reduced in the proportion of the coarse material at prescreening.

As indicated in the introduction, the energy register of any comminution step is calculated from the accumulated specific energy of the successive previous size reduction steps. These values are assigned to the mass specific surface of the respective comminution product and build up the energy register diagram. In all the analyzed cases the succession of points can be well approximated by a straight line. The inclination of the linear approximation defines the Rittinger coefficient.

The energy register of the first comminution product (1st crushing stage) was obtained by shifting the origin into the intersection of the linear extrapolation with the abscissa.

# 8. RESULTS

The summarized results of the mass specific net energy consumption related to the non-fragmented state of the sample (energy registers) as well as the mass specific surface of the products out of energy optimized comminution are supplied in Table 7. The first energy value is deduced from linear extrapolation, all the others are based on measurements. Figure 20 shows the plot of the energy registers versus mass specific surface of all the samples. The correlation coefficients (> 99.5%) justify the linear approximation of the data.

**Table 7: Summarized energy registers and Rittinger coefficients**

| comminution stage | Hengl-Bitustein | | Cementos Portland | | Nordkalk R | | Nordkalk S | | Nordkalk K | | Nordkalk F | |
|---|---|---|---|---|---|---|---|---|---|---|---|---|
| | $\Sigma\Delta e$ [J/g] | $a_M$ [cm²/g] | $\Sigma\Delta e$ [J/g] | $a_M$ [cm²/g] | $\Sigma\Delta e$ [J/g] | $a_M$ [cm²/g] | $\Sigma\Delta e$ [J/g] | $a_M$ [cm²/g] | $\Sigma\Delta e$ [J/g] | $a_M$ [cm²/g] | $\Sigma\Delta e$ [J/g] | $a_M$ [cm²/g] |
| 100% < 40mm | 0,17 | 27 | 0,07 | 31 | 0,44 | 55 | 0,54 | 57 | 0,58 | 53 | 1,12 | 104 |
| 100% <16mm | 2,84 | 91 | 1,84 | 102 | 1,95 | 132 | 2,15 | 136 | 2,06 | 166 | 1,98 | 212 |
| 100% <6,3mm | 6,75 | 214 | 4,10 | 236 | 4,31 | 264 | 4,18 | 276 | 4,86 | 404 | 3,26 | 380 |
| 100% <3,15mm | 11,29 | 360 | 7,52 | 407 | 7,27 | 427 | 6,76 | 434 | 7,69 | 595 | 4,91 | 527 |
| 100% <1mm | 15,97 | 567 | 13,42 | 819 | 12,48 | 844 | 11,03 | 758 | 11,66 | 963 | 7,87 | 842 |
| Rittinger coefficient, cm²/J | 34 | | 59 | | 65 | | 67 | | 81 | | 108 | |
| Correlation Coefficient, % | 99,61 | | 99,7 | | 99,58 | | 99,85 | | 99,91 | | 99,88 | |

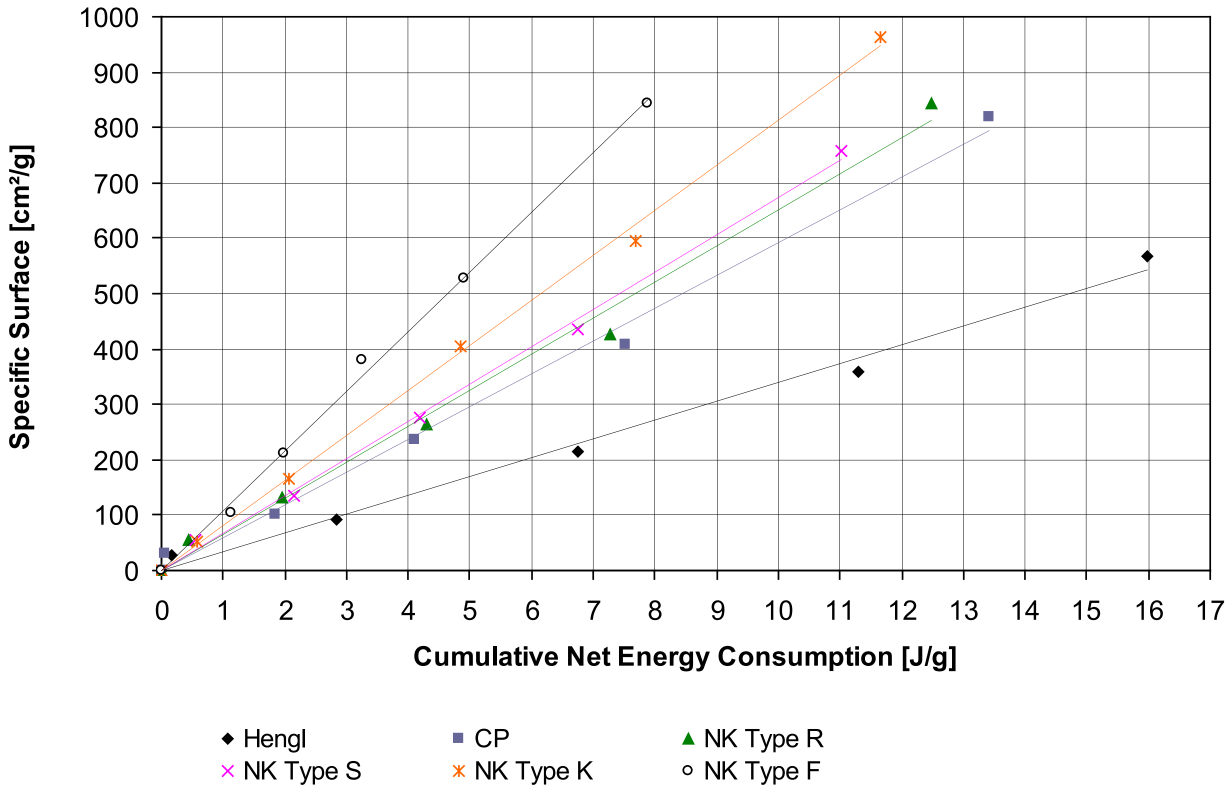


**Figure 20: Energy register functions of the six rock samples: amphibolite Hengl (Hengl), limestone Cementos Portland (CP), limestone Nordkalk (NK) types R, S, K, and F**

The Natural Breakage Characteristic of a given mineral material is defined as the particle size distribution with the smallest variation of particle size classes at a given maximum particle size. Independent from the comminution tool all its NBC-curves display self-similarity indicated by the parallel shift along the ordinate at least in the fines' range below 1 mm. The size class -1 mm contains more than 90% of the specific surface, reflecting the supplied energy for comminution.

The NBC curves of the supplied samples are depicted in Figures 21 to 26.

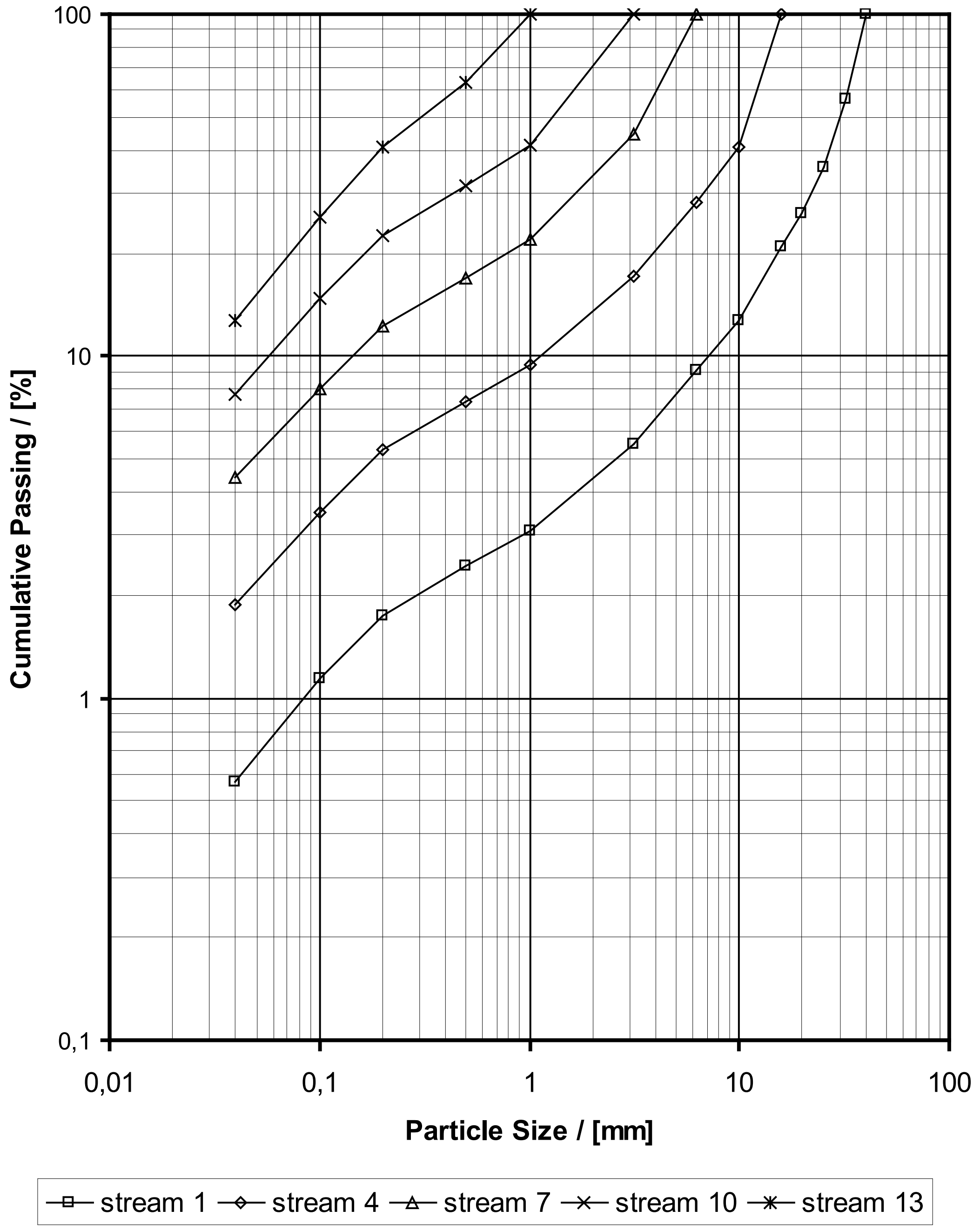


| | |
|---|---|
| Amphibolite, Hengl Bitustein<br>Sample no.: Less Fines 1<br>Particle size distributions<br>of the streams 1, 4, 7, 10, 13 | GGS - grid |

**Figure 21: NBC particle size distributions of the sample Hengl-Bitustein**

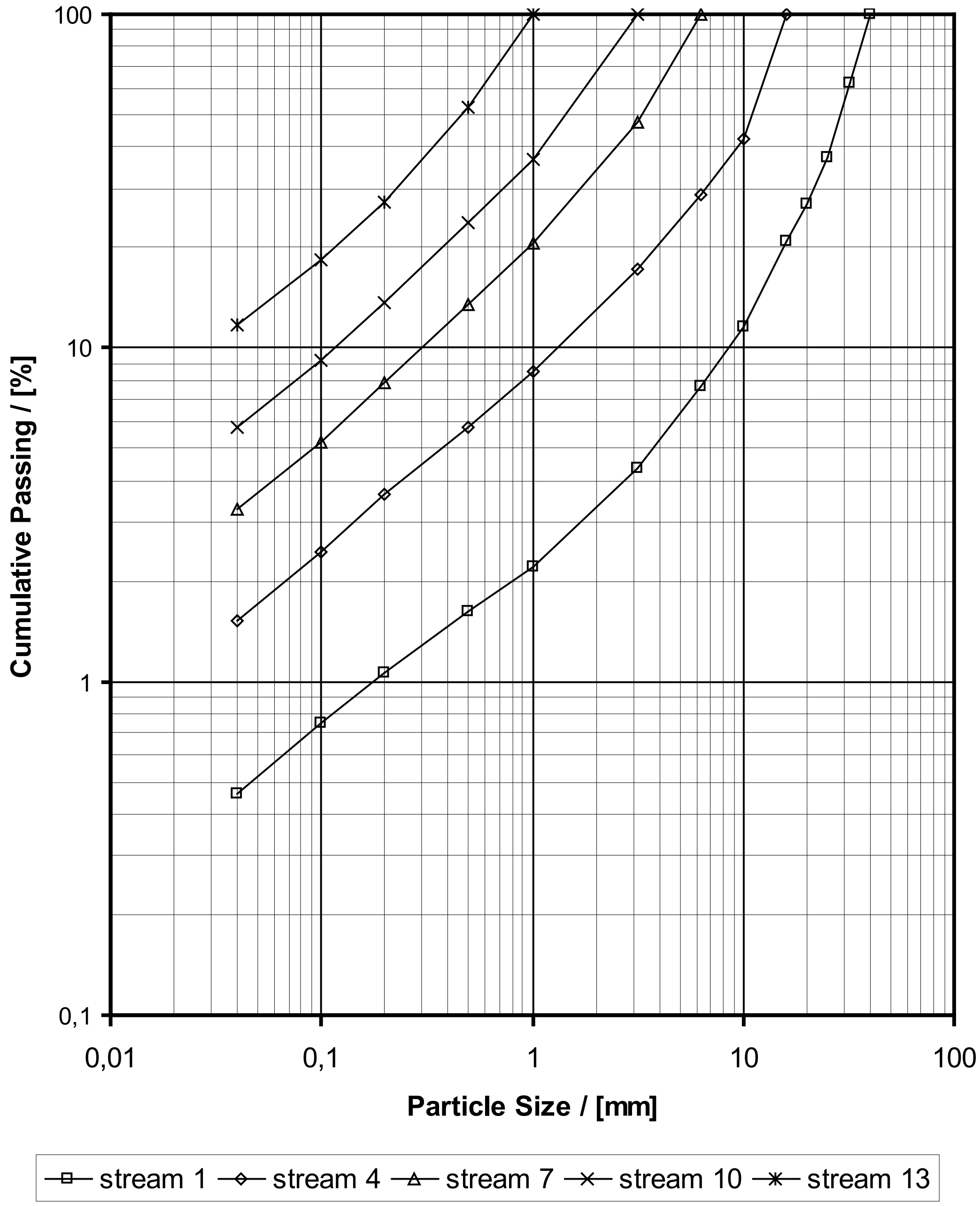


| | |
|---|---|
| Limestone, Cementos Portland<br>Sample no.: Less Fines 2<br>Particle size distributions<br>of the streams 1, 4, 7, 10, 13 | GGS - grid |

**Figure 22: NBC particle size distributions of the sample Cementos Portland**

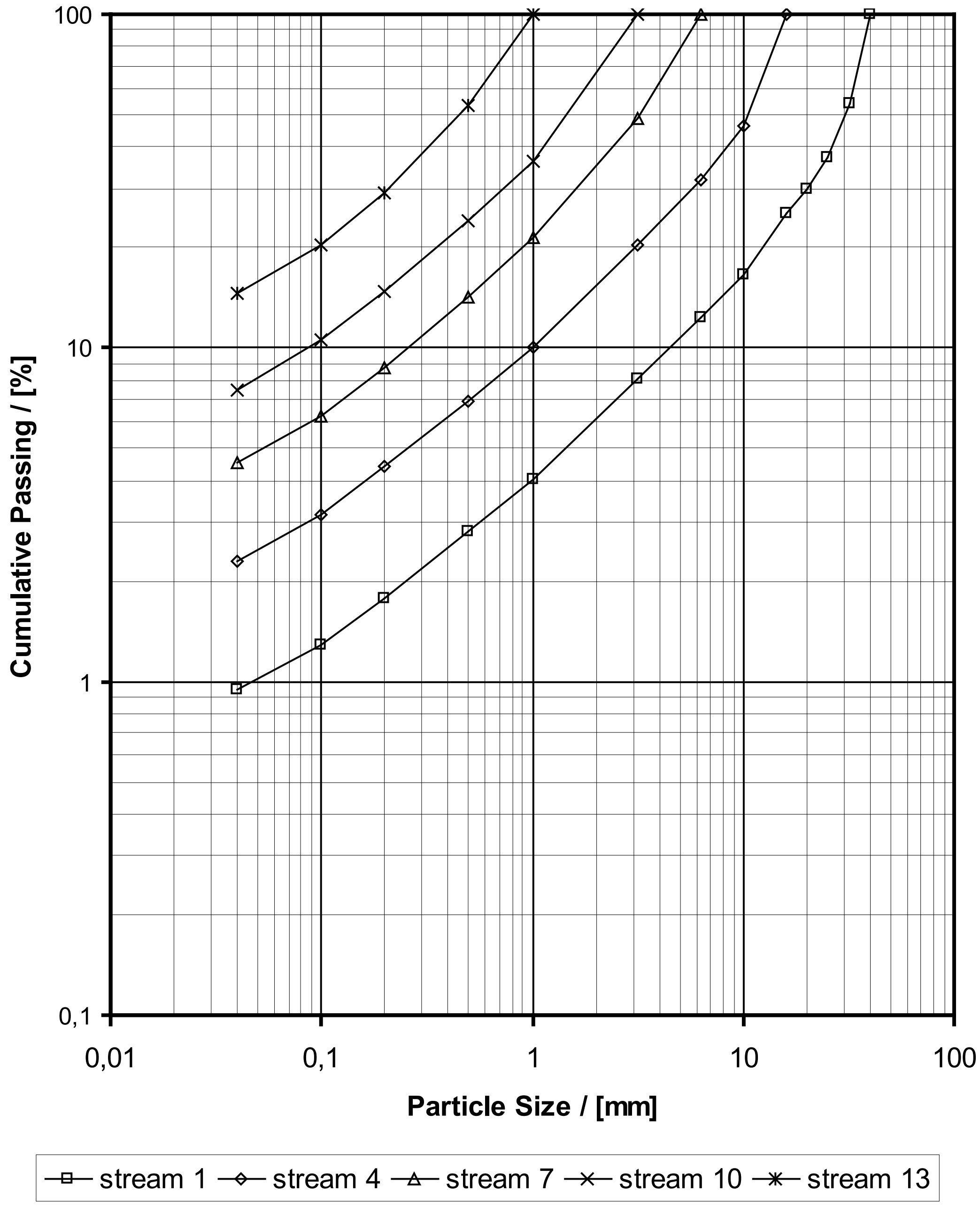


| | |
|---|---|
| Limestone, Nordkalk, Type R<br>Sample no.: Less Fines 3<br>Particle size distributions<br>of the streams 1, 4, 7, 10, 13 | GGS - grid |

**Figure 23: NBC particle size distributions of the sample Nordkalk R**

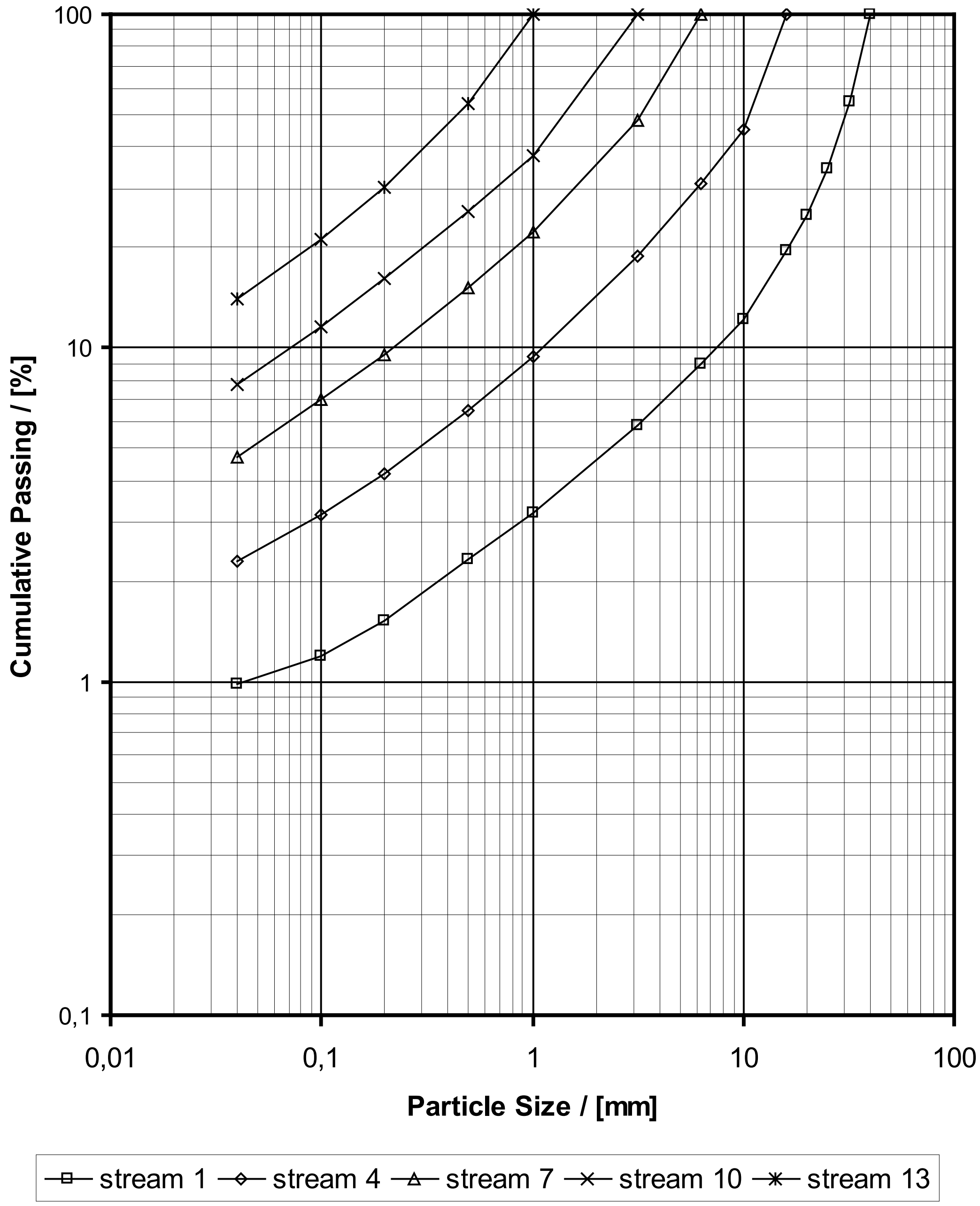


| | |
|---|---|
| Limestone, Nordkalk, Type S<br>Sample no.: Less Fines 4<br>Particle size distributions<br>of the streams 1, 4, 7, 10, 13 | GGS - grid |

**Figure 24: NBC particle size distributions of the sample Nordkalk S**

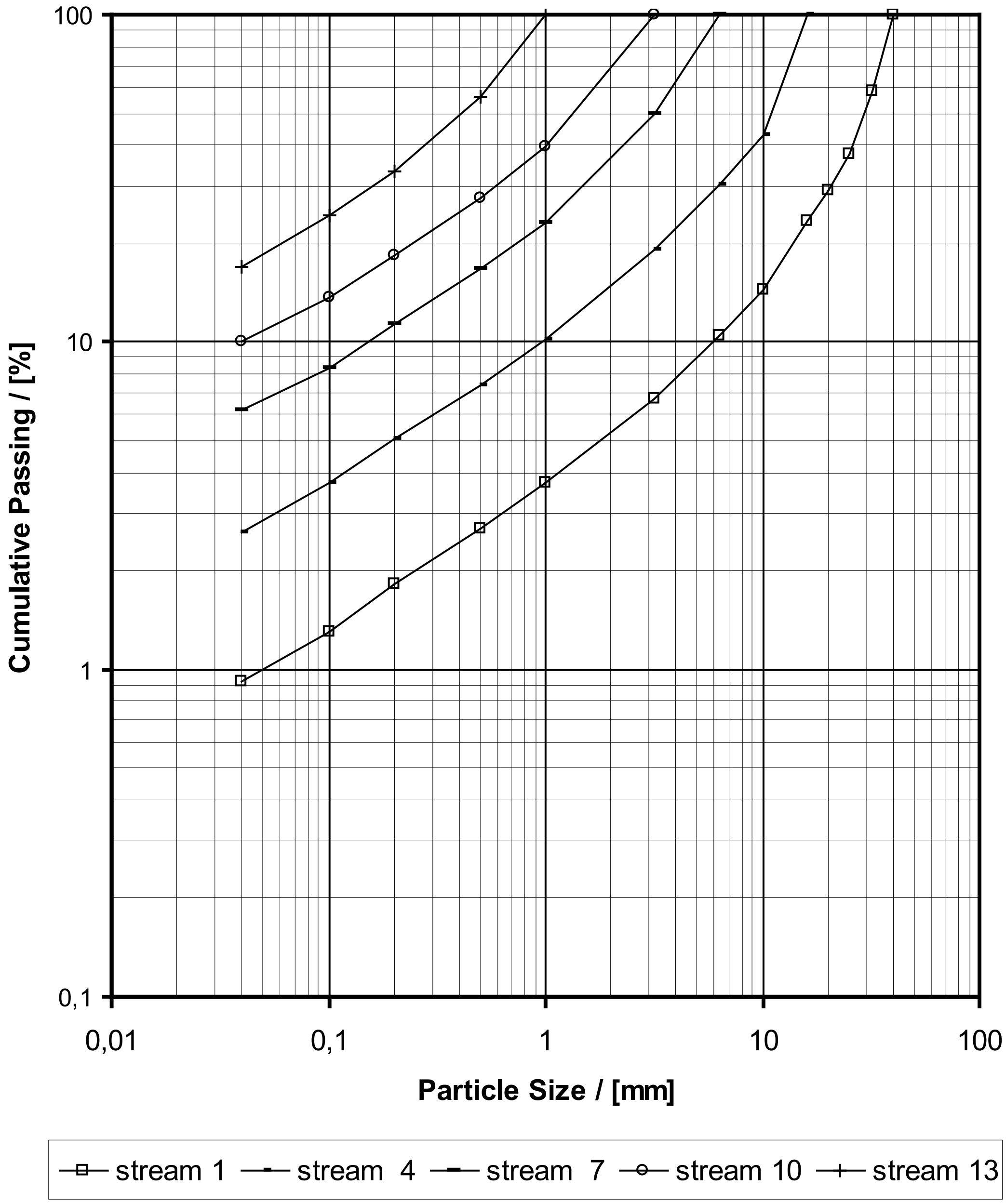


| | |
|---|---|
| Limestone, Nordkalk, Type K<br>Sample no.: Less Fines 5<br>Particle size distributions<br>of the streams 1, 4, 7, 10, 13 | GGS - grid |

**Figure 25: NBC particle size distributions of the sample Nordkalk K**

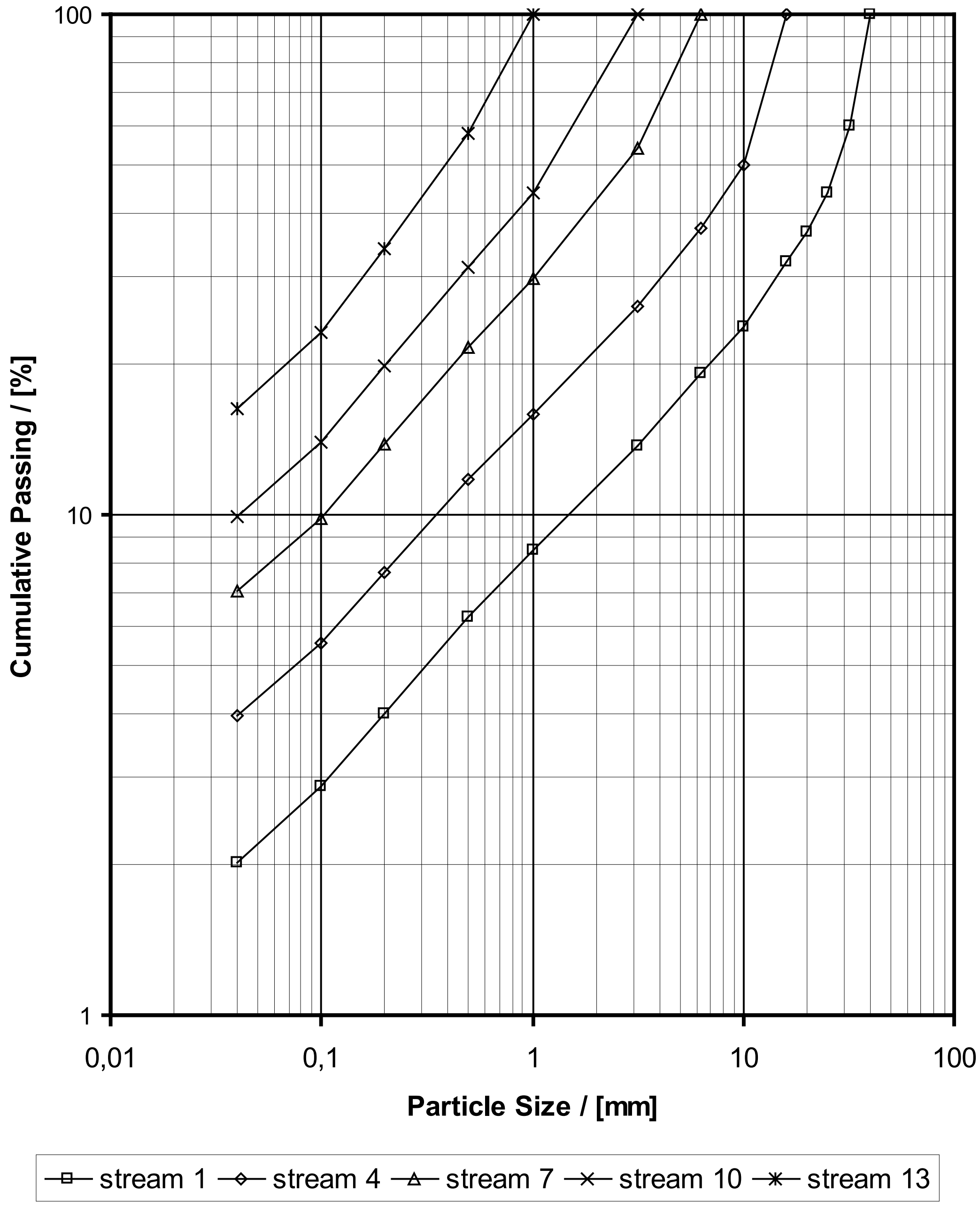


| | |
|---|---|
| Limestone, Nordkalk, Type F<br>Sample no.: Less Fines 6<br>Particle size distributions<br>of the streams 1, 4, 7, 10, 13 | GGS - grid |

**Figure 26: NBC particle size distributions of the sample Nordkalk F**

# REFERENCES

[1] Steiner, H.J.: Zerkleinerungstechnische Eigenschaften von Gesteinen, Sonderdruck aus Felsbau 16, no.5, 1998, p 320-325

[2] Steiner, H.J.: The significance of the Rittinger equation in present-day comminution technology, Proceedings of the XVIIth International Mineral Processing Congress, Dresden 1991, Vol. 1. Polygraphischer Bereich, Bergakademie Freiberg/Sa, Freiberg, 1991, p 177-188

[3] Steiner, H.J.: Characterization of laboratory-scale tumbling mills, Int. J. Miner. Process. 44-45, 1996, p 373-382

[4] Steiner, H.J.: Rahmengesetzmäßigkeiten der natürlichen Bruchcharakteristik von Mineralen und Gesteinen, Erzmetall 43, no. 10, 1990, p 435-440